



NRL/MR/6930--18-9808

Colorimetric Environmental Sensor: Aqueous Indicator Screening (Part 2)

BRANDY J. WHITE
MARTIN H. MOORE

*Laboratory for the Study of Molecular Interfacial Interactions
Center for Bio/Molecular Science & Engineering*

KALEB FRANCO
*Forest Park High School
Woodbridge, VA*

ANTHONY P. MALANOSKI
*Laboratory for Biosensors and Biomaterials
Center for Bio/Molecular Science & Engineering*

September 17, 2018

REPORT DOCUMENTATION PAGE				Form Approved OMB No. 0704-0188	
Public reporting burden for this collection of information is estimated to average 1 hour per response, including the time for reviewing instructions, searching existing data sources, gathering and maintaining the data needed, and completing and reviewing this collection of information. Send comments regarding this burden estimate or any other aspect of this collection of information, including suggestions for reducing this burden to Department of Defense, Washington Headquarters Services, Directorate for Information Operations and Reports (0704-0188), 1215 Jefferson Davis Highway, Suite 1204, Arlington, VA 22202-4302. Respondents should be aware that notwithstanding any other provision of law, no person shall be subject to any penalty for failing to comply with a collection of information if it does not display a currently valid OMB control number. PLEASE DO NOT RETURN YOUR FORM TO THE ABOVE ADDRESS.					
1. REPORT DATE (DD-MM-YYYY) 17-09-2018		2. REPORT TYPE Memorandum Report		3. DATES COVERED (From - To) 9/30/2013-08/01/2018	
4. TITLE AND SUBTITLE Colorimetric Environmental Sensor: Aqueous Indicator Screening (Part 2)				5a. CONTRACT NUMBER	
				5b. GRANT NUMBER	
				5c. PROGRAM ELEMENT NUMBER	
6. AUTHOR(S) Brandy J. White, Martin H. Moore, Kaleb Franco* and Anthony P. Malanoski				5d. PROJECT NUMBER	
				5e. TASK NUMBER	
				5f. WORK UNIT NUMBER 69-6594	
7. PERFORMING ORGANIZATION NAME(S) AND ADDRESS(ES) Center for Bio/Molecular Science & Engineering Naval Research Laboratory 4555 Overlook Avenue, SW Washington, DC 20375-5344				8. PERFORMING ORGANIZATION REPORT NUMBER NRL/MR/6930--18-9808	
9. SPONSORING / MONITORING AGENCY NAME(S) AND ADDRESS(ES)				10. SPONSOR / MONITOR'S ACRONYM(S) NRL 6.2	
				11. SPONSOR / MONITOR'S REPORT NUMBER(S)	
12. DISTRIBUTION / AVAILABILITY STATEMENT DISTRIBUTION STATEMENT A: Approved for public release; distribution is unlimited.					
13. SUPPLEMENTARY NOTES *KF SEAP: Forest Park High School, Woodbridge, VA					
14. ABSTRACT This report is work focused on a component of an effort intended to develop wireless sensor networks for real-time monitoring of airborne targets across a broad area. The performance of the sensor devices will depend heavily on the selection of appropriate indicator elements in design of the arrays. This document summarizes results for aqueous screening of meso-tetra(4-carboxyphenyl) porphyrin (C4TPP) and metalloporphyrin (XC4TPP) variants of this structure.					
15. SUBJECT TERMS environmental sensor, chemical sensor, colorimetric, porphyrin					
16. SECURITY CLASSIFICATION OF:			17. LIMITATION OF ABSTRACT Unclassified Unlimited	18. NUMBER OF PAGES 26	19a. NAME OF RESPONSIBLE PERSON Brandy J. White
a. REPORT Unclassified Unlimited	b. ABSTRACT Unclassified Unlimited	c. THIS PAGE Unclassified Unlimited			19b. TELEPHONE NUMBER (include area code) (202) 404-6100

This page intentionally left blank.

CONTENTS

INTRODUCTION	1
METHODS	1
RESULTS	2
CONCLUSIONS.....	5
REFERENCES	5
APPENDIX A – ABSORBANCE DATA	6

FIGURES

Fig. 1	— Porphyrin molecular structures	1
Fig. 2	— Absorbance spectra of porphyrin	2
Fig. 3	— Absorbance and difference absorbance spectra	3
Fig. 4	— Concentration dependence	3
Fig. 5	— Affinity coefficients	5

TABLES

Table 1	— Fitting parameters	4
---------	----------------------------	---

EXECUTIVE SUMMARY

In October 2012, the Center for Bio/Molecular Science and Engineering at the Naval Research Laboratory (NRL) began an effort intended to develop wireless sensor networks for real-time monitoring of airborne targets across a broad area. The goal was to apply the spectrophotometric characteristics of porphyrins and metalloporphyrins in a colorimetric array for detection and discrimination of changes in the chemical composition of environmental air samples. The performance of the device will depend heavily on the selection of appropriate indicator elements in design of the arrays. The current document summarizes results for aqueous screening of meso-tetra(4-carboxyphenyl) porphyrin (C₄TPP) and metalloporphyrin (XC₄TPP) variants of this structure.

This page intentionally left blank.

COLORIMETRIC ENVIRONMENTAL SENSOR: AQUEOUS INDICATOR SCREENING

INTRODUCTION

In October 2012, the Center for Bio/Molecular Science and Engineering at the Naval Research Laboratory (NRL) began an effort (69-6594) intended to develop wireless sensor networks for real-time monitoring of airborne targets across a broad area. The goal was to apply the spectrophotometric characteristics of porphyrins and metalloporphyrins in a colorimetric array for detection and discrimination of changes in the chemical composition of environmental air samples. The effort encompasses hardware, software, and firmware development as well as development of algorithms for identification of event occurrence and discrimination of targets. [1, 2, 3, 4] The performance of these components is dependent on selection of the appropriate indicator elements in design of the array. The current document summarizes results for aqueous screening of meso-tetra(4-carboxyphenyl) porphyrin (C₄TPP) and metalloporphyrin (XC₄TPP) variants of this structure (Figure 1).

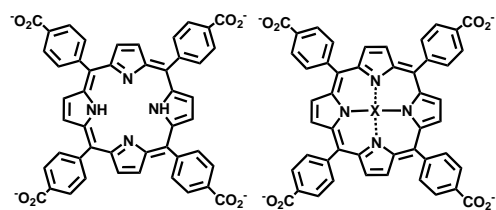


Fig. 1 — Molecular structures of meso-tetra(4-carboxyphenyl) porphyrin (C₄TPP) and the metalloporphyrin (XC₄TPP) variants of this structure.

The targets utilized in the evaluation of these indicator materials are ethanol, methanol, and isopropanol. These targets were selected for prototype development because they present a low degree of hazard allowing for their use in a range of environments and scenarios while providing the potential for evaluation of the full sensor package. The screening approach uses aqueous solutions of the porphyrins to which varying concentrations of the alcohols are added. The changes in absorbance allow for calculation of affinity coefficients. The expectation is that the affinity coefficient between the target and indicator will be related to the sensitivity of the paper supported indicator for that target.

METHODS

Meso-tetra(4-carboxyphenyl) porphyrin (C₄TPP) was obtained from Frontier Scientific (Logan, UT). Metalloporphyrin variants of C₄TPP were prepared by reflux. [1, 2, 3] The porphyrin (20 mg) was dissolved in 2 mL water with sodium hydroxide (sufficient only to dissolve the porphyrin full). The metal salt was added to this solution in a 3:1 molar ratio with the porphyrin. The total volume was brought to 100 mL with deionized water and refluxed overnight. The volume of the resulting solution was reduced to 20 mL through rotary evaporation. Prepared metal salt solutions were stored in the dark at room temperature. The metal salts used here were: yttrium (III) chloride, iron (II) sulfate, nickel (II) chloride, zinc chloride, copper (II) chloride, cadmium chloride, cerium (III) chloride, silver chloride, and cobalt (II) chloride.

Absorbance spectra of the porphyrin solutions were collected using an Agilent 8453 UV/vis spectrophotometer (Agilent Technologies, Inc., Santa Clara, CA) from 190 to 1100 nm at 2 nm resolution. Solutions were prepared in a quartz cuvette using deionized water (18.2 MΩ; 3 mL) and 10 μL of the prepared porphyrin solution (2 mg/mL, above). The absorbance spectrum of this as prepared solution was compared to that of the same solution amended with ethanol, methanol, or isopropanol added in 10 μL aliquots. Final concentrations are indicated in the text and figure captions.

RESULTS

A series of metalloporphyrin variants were prepared based on the C₄TPP structure. Absorbance spectra of these variants were collected in aqueous solution (Figure 2). The absorbance of the porphyrin (or metalloporphyrin) in aqueous solution was used as a point of comparison for the absorbance spectra of the same solution amended with ethanol, methanol, or isopropanol (Figure 3). Ethanol concentrations were increased through sequential addition of 10 μL aliquots for final concentrations of 57, 113, 169, 225, 280, 335, 390, and 444 mM. The same series were collected for isopropanol with final concentrations of 43, 86, 129, 171, 214, 256, 298, and 339 mM and for methanol with final concentrations of 82, 163, 244, 325, 404, 483, 563, and 641 mM (Figure 3; full data set provided in Appendix A). The porphyrin concentration was 9.86 μM in the initial solution. Absorbance spectra have been corrected for dilution resulting from target addition. Difference spectra were calculated as the point by point subtraction of the porphyrin + alcohol minus the porphyrin solution alone (Figure 3).

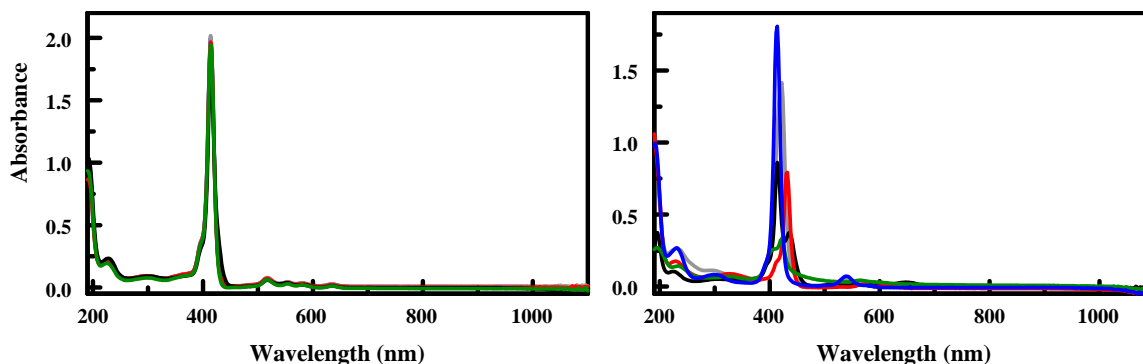


Fig. 2 — Absorbance spectra of the porphyrin and metalloporphyrin variants considered (9.86 μM in water): (left) CoC₄TPP (black), CeC₄TPP (red), FeC₄TPP (green), NiC₄TPP (blue), YC₄TPP (gray); (right) CdC₄TPP (red), ZnC₄TPP (green), AgC₄TPP (gray), C₄TPP (black), CuC₄TPP (blue).

The difference spectra (Figure 3) were used to identify peak and trough positions for additional analysis. The change in absorbance for the characteristic peak / trough positions were plotted versus target concentration (Figure 4). Fitting parameters were determined based on an expression that combines the standard form of a binding interaction and the Beer-Lambert Law. This approach assumes: (1) the porphyrin-analyte complex is 1:1; (2) Beer's Law is followed by the porphyrin, analyte, and the porphyrin-analyte complex; and (3) the extinction coefficients of the free reagents at the wavelength under consideration are significantly different from that of the porphyrin-analyte complex. The resulting expression provides the relationship between the absorbance change (ΔA) and the variables porphyrin concentration ($[P]$), analyte concentration ($[L]$), and complex stability constant (K_{11}).

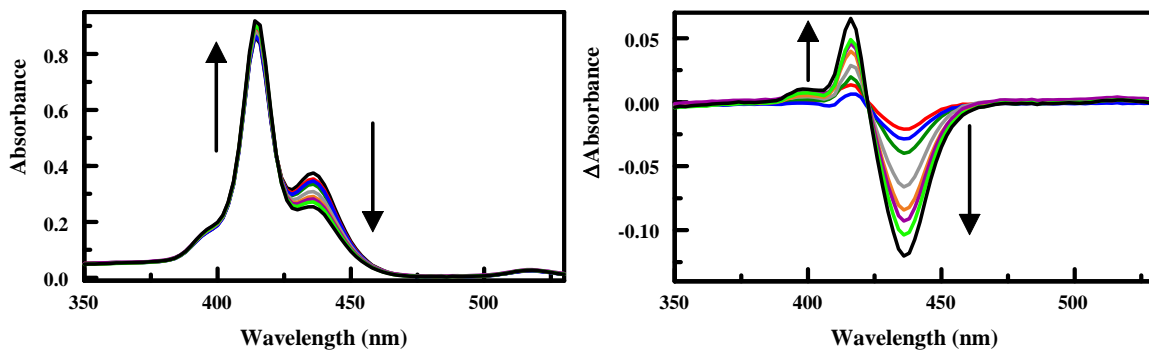


Fig. 3 — Absorbance spectra of C₄TPP (9.86 μM; left) in the absence and presence of increasing concentrations of ethanol: 57, 113, 169, 225, 280, 335, 390, and 444 mM. Arrows indicate increasing target concentration. Absorbance spectra have been corrected for dilution resulting from target addition. Difference absorbance spectra (right) are calculated as porphyrin + target minus porphyrin.

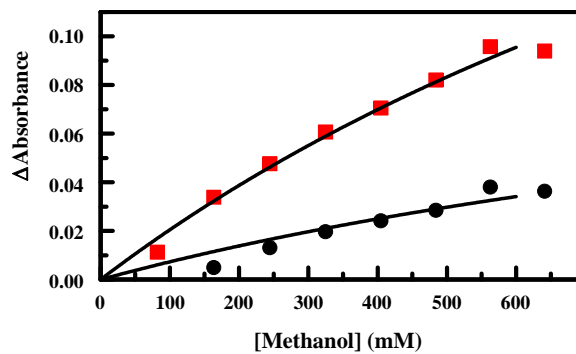


Fig. 4 — The concentration dependence of features in the C₄TPP absorbance spectra is presented for methanol exposures. Here, the change in absorbance at the peak (418 nm, black) and trough (436 nm, red) is plotted against target concentration. Lines are the result of fitting the expression to this data set.

Derivation of the final expression begins with the Beer-Lambert Law stating:

$$A_0 = \epsilon_P b [P_t]$$

where A_0 is the initial absorbance of the porphyrin, $[P_t]$ is the total porphyrin concentration, ϵ_P is the extinction coefficient at the wavelength under consideration, and b is the path length for the measurement. In the presence of analyte (total concentration $[L_t]$), the absorbance of a solution containing the same total porphyrin concentration is:

$$A_L = \epsilon_P b [P] + \epsilon_L b [L] + \epsilon_{11} b [PL].$$

Here, ϵ_L and ϵ_{11} are the extinction coefficients of the analyte and the complex, respectively, and $[PL]$ is the concentration of the complex. If the reference spectrum is taken against a ligand spectrum at $[L_t]$ or the ligand does not absorb in the considered region, this expression becomes:

$$A_L = \epsilon_P b [P] + \epsilon_{11} b [PL].$$

The change in absorbance upon addition of ligand is then:

$$\Delta A = \epsilon_P b [P] + \epsilon_{11} b [PL] - \epsilon_P b P_t$$

Recalling that $P_t = [P] + [PL]$ and defining $\Delta\epsilon_{11} = \epsilon_{11} - \epsilon_P$, the expression can be rewritten:

$$\Delta A = \Delta\epsilon_{11} b [PL]$$

The standard binding isotherm is of the form:

$$[PL] = \frac{[P_t] K [L]}{1 + K [L]}$$

yielding a final expression of:

$$\Delta A = \Delta \varepsilon_{11} b \frac{[P_t]K[L]}{1 + K[L]}$$

Here, $[L_t] \gg [P_t]$, so we can approximate $[L] = [L_t]$.

Fitting parameters for the data sets are provided in Table 1. Fits were based on two wavelengths identified based on the prominent features in the difference spectra. The determined difference extinction coefficients varied across three orders of magnitude with the iron metal complex yielding the lowest values and the copper and porphyrin alone variants yielding the largest values. Extinction coefficients may have some impact on the performance of indicator materials in the final devices; however, some of this difference may be corrected through increasing the porphyrin loading in the supported indicator system. In addition, the prototype devices use the full spectrum of reflected light, rather than absorbance at a single wavelength. The affinity coefficients are expected to provide a more valuable point of comparison; these are summarized in Figure 5. If all extinction coefficients were equal, a larger affinity coefficient would provide a larger change in absorbance for a given indicator and target concentration.

Table 1 – Fit Parameters for the Porphyrin Indicators

Porphyrin	Target	K (mM ⁻¹)	Wavelength (nm)	$\Delta \varepsilon_{11}$ (mM ⁻¹ ·cm ⁻¹)	Wavelength (nm)	$\Delta \varepsilon_{11}$ (mM ⁻¹ ·cm ⁻¹)
C4TPP	Ethanol	6.56E-6	416	2083	436	4247
	Isopropanol	3.02E-3	418	8.15	436	28.80
	Methanol	6.07E-4	418	12.96	436	36.28
AgC4TPP	Ethanol	5.10E-3	422	16.82	441	1.28
	Isopropanol	5.99E-3	420	8.15	439	2.33
	Methanol	7.12E-4	420	26.86	440	4.58
CdC4TPP	Ethanol		--		--	
	Isopropanol	2.56E-5	408	1.30	430	526.9
	Methanol	8.90E-5	408	1.87	430	76.57
CeC4TPP	Ethanol	2.73E-4	408	57.35	422	25.31
	Isopropanol	5.12E-4	410	75.72	424	30.59
	Methanol		408		430	
CoC4TPP	Ethanol	1.20E-3	412	12.67	420	11.64
	Isopropanol	6.82E-4	410	49.75	422	21.37
	Methanol		412		422	
CuC4TPP	Ethanol	2.06E-3	404	2.76	414	6.65
	Isopropanol	4.51E-6	402	1063	424	1240
	Methanol	7.92E-6	406	345.5	422	81.29
FeC4TPP	Ethanol	1.60E-4	408	94.34	424	33.25
	Isopropanol	5.08E-5	410	73.92	424	29.92
	Methanol	2.88E-3	412	10.84	424	2.60
NiC4TPP	Ethanol	5.16E-4	407	24.74	421	18.72
	Isopropanol	4.21E-4	411	76.76	422	43.02
	Methanol	4.49E-2	414	19.70	392	4.87
YC4TPP	Ethanol	5.61E-6	412	4963	434	1093
	Isopropanol	4.41E-6	412	7911	420	4052
	Methanol	9.08E-6	410	969	426	160
ZnC4TPP	Ethanol	4.21E-2	388	0.42	422	19.56
	Isopropanol	2.48E-2	390	0.53	424	7.32
	Methanol	2.10E-2	392	0.87	422	16.02

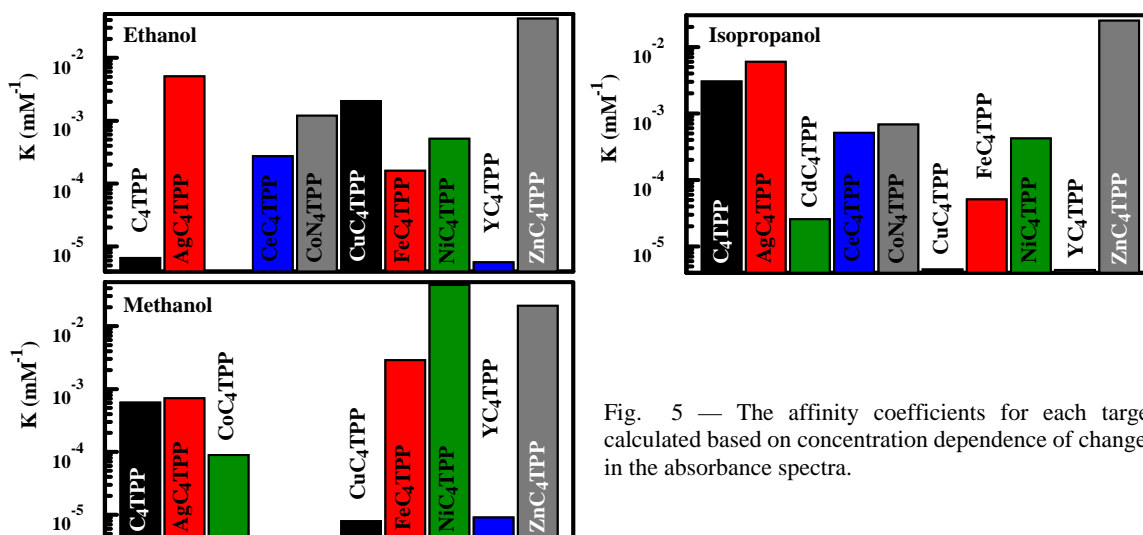


Fig. 5 — The affinity coefficients for each target calculated based on concentration dependence of changes in the absorbance spectra.

CONCLUSIONS

The data provided here is an initial study intended to support development of indicator arrays for use in the NRL prototype environmental sensor system. The meso-tetra(4-carboxyphenyl) porphyrin (C₄TPP) variants are sensitive to the alcohol model targets. Different metal complexes demonstrate widely varying affinities and changes in extinction coefficient upon interaction with the targets. The ongoing effort will screen additional porphyrin structures, including meso-tetra(4-sulfonatophenyl) porphyrin (S₄TPP) and meso-tetra(4-aminophenyl) porphyrin (N₄TPP). Additional work will also provide data on screening of the paper supported versions of these indicators. The overall goal is to design an array of elements that provide the potential for discrimination of targets based on the relative response of the individual elements.

ACKNOWLEDGEMENTS

K. Franco was at NRL during the summer of 2018 through the Office of Naval Research (ONR) Science & Engineering Apprenticeship Program (SEAP).

REFERENCES

1. B.J. Johnson; J.S. Erickson; J. Kim; A.P. Malanoski; I.A. Leska; S.M. Monk; D.J. Edwards; T.N. Young; J. Verbarg; C. Bovais; R.D. Russell; D.A. Stenger, "Miniaturized reflectance devices for chemical sensing," *Meas. Sci. Technol.* **25**, 095101 (2014).
2. B.J. Johnson; R. Liu; R.C. Neblett; A.P. Malanoski; M. Xu; J.S. Erickson; L. Zang; D.A. Stenger; M.H. Moore, "Reflectance-based detection of oxidizers in ambient air," *Sens. Actuator B-Chem.* **227**, 399-402 (2016).
3. A.P. Malanoski; B.J. Johnson; J.S. Erickson; D.A. Stenger, "Development of a Detection Algorithm for Use with Reflectance-Based, Real-Time Chemical Sensing," *Sensors* **16**, 1927 (2016).
4. B.J. Johnson; A.P. Malanoski; J.S. Erickson; R. Liu; A.R. Remenapp; D.A. Stenger; M.H. Moore, "Reflectance-based detection for long term environmental monitoring," *Heliyon* **3**, e00312 (2017).

Appendix A

ABSORBANCE DATA

Figure A-1. Absorbance spectra (top) of C₄TPP (9.86 μ M) in the absence and presence of increasing concentrations of ethanol: 57, 113, 169, 225, 280, 335, 390, and 444 mM. Arrows indicate increasing target concentration. Absorbance spectra have been corrected for dilution resulting from target addition. Difference absorbance spectra (bottom) are calculated as porphyrin + target minus porphyrin. The concentration dependence of features in the absorbance spectra is also presented (right). Here, the change in absorbance at the peak and trough positions (416 and 436 nm) is plotted against target concentration.

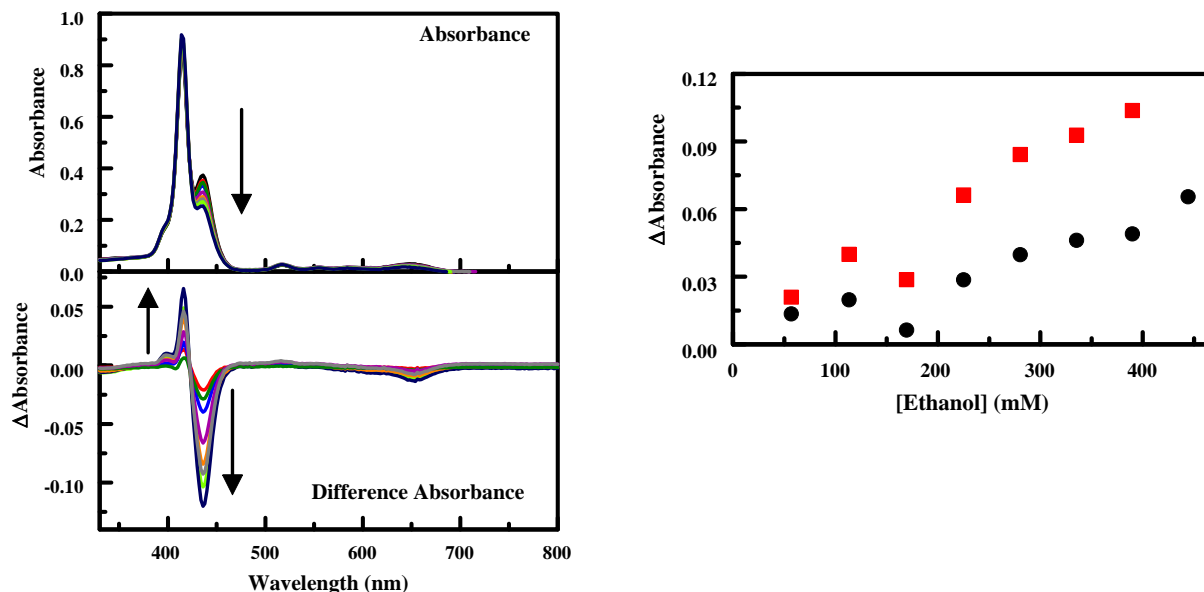


Figure A-2. Absorbance spectra (top) of C₄TPP (9.86 μ M) in the absence and presence of increasing concentrations of isopropanol: 43, 86, 129, 171, 214, 256, 298, and 339 mM. Arrows indicate increasing target concentration. Absorbance spectra have been corrected for dilution resulting from target addition. Difference absorbance spectra (bottom) are calculated as porphyrin + target minus porphyrin. The concentration dependence of features in the absorbance spectra is also presented (right). Here, the change in absorbance at the peak and trough positions (418 and 436 nm) is plotted against target concentration.

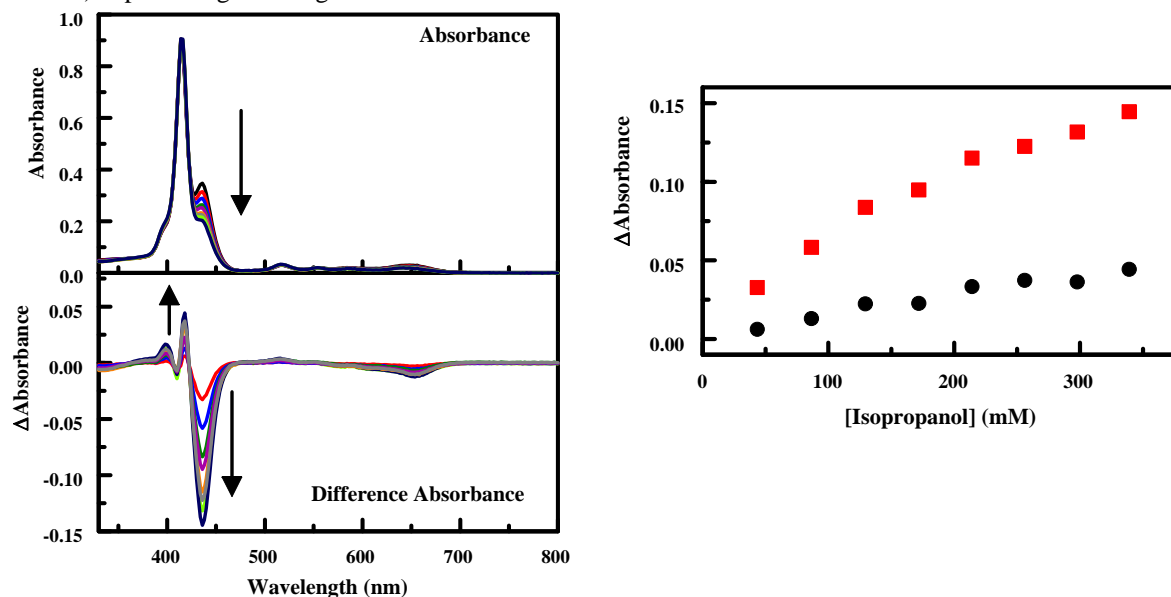


Figure A-3. Absorbance spectra (top) of C₄TPP (9.86 μ M) in the absence and presence of increasing concentrations of methanol: 82, 163, 244, 325, 404, 483, 563, and 641 mM. Arrows indicate increasing target concentration. Absorbance spectra have been corrected for dilution resulting from target addition. Difference absorbance spectra (bottom) are calculated as porphyrin + target minus porphyrin. The concentration dependence of features in the absorbance spectra is also presented (right). Here, the change in absorbance at the peak and trough positions (416 and 436 nm) is plotted against target concentration.

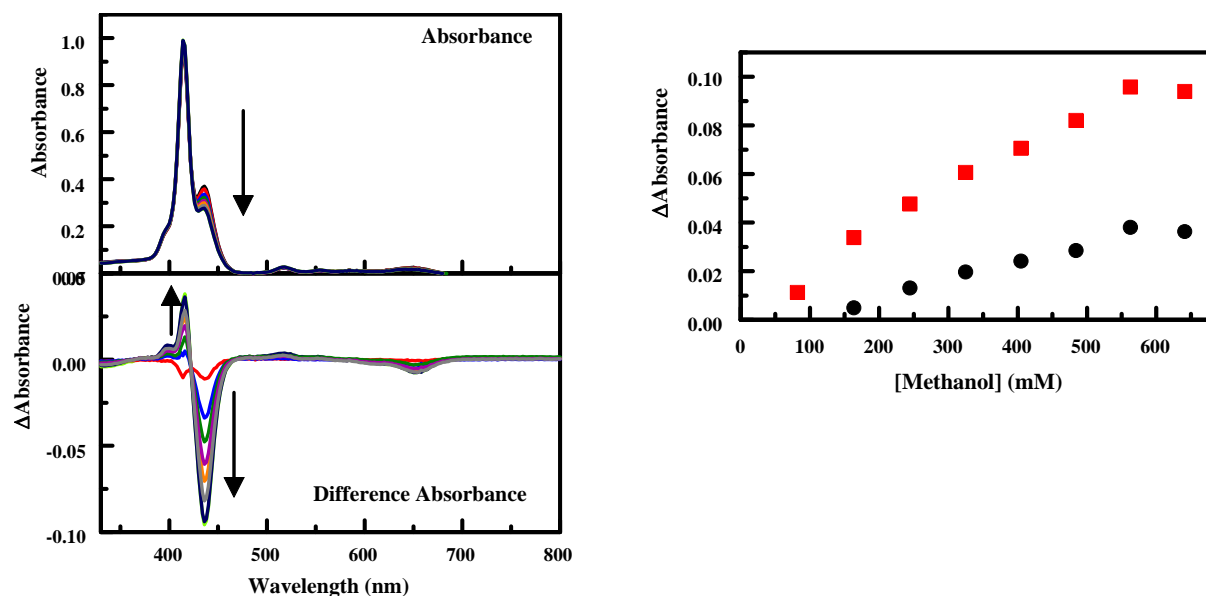


Figure A-4. Absorbance spectra (top) of AgC₄TPP (9.86 μ M) in the absence and presence of increasing concentrations of ethanol: 57, 113, 169, 225, 280, 335, 390, and 444 mM. Arrows indicate increasing target concentration. Absorbance spectra have been corrected for dilution resulting from target addition. Difference absorbance spectra (bottom) are calculated as porphyrin + target minus porphyrin. The concentration dependence of features in the absorbance spectra is also presented (right). Here, the change in absorbance at the trough positions (422 and 441 nm) is plotted against target concentration.

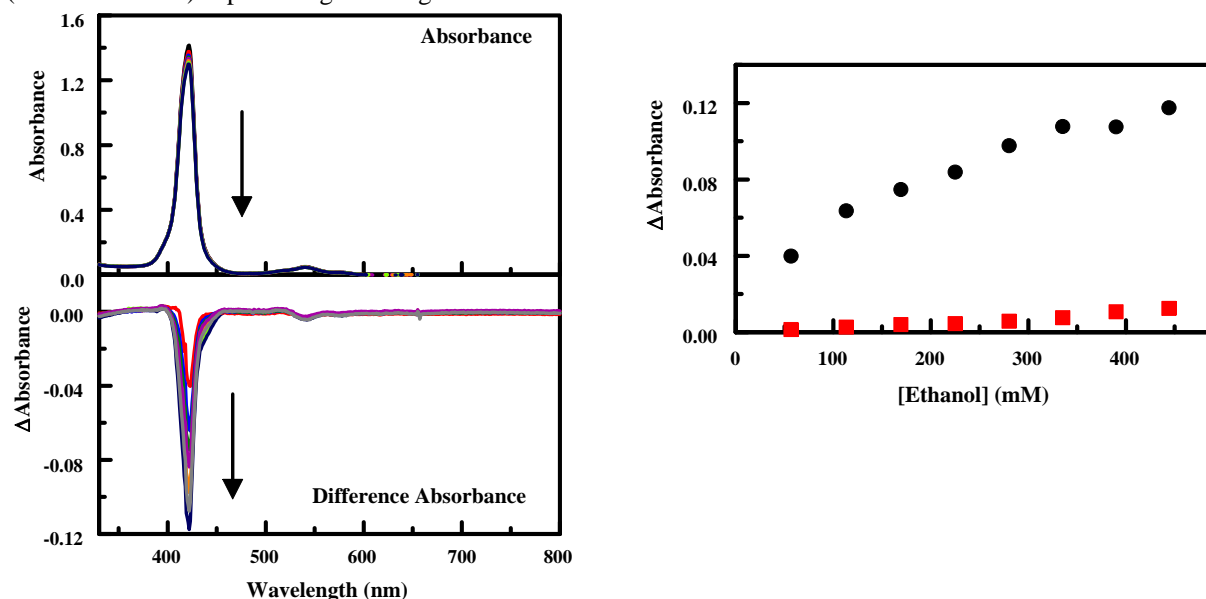


Figure A-5. Absorbance spectra (top) of AgC₄TPP (9.86 μ M) in the absence and presence of increasing concentrations of isopropanol: 43, 86, 129, 171, 214, 256, 298, and 339 mM. Arrows indicate increasing target concentration. Absorbance spectra have been corrected for dilution resulting from target addition. Difference absorbance spectra (bottom) are calculated as porphyrin + target minus porphyrin. The concentration dependence of features in the absorbance spectra is also presented (right). Here, the change in absorbance at the trough positions (420 and 439 nm) is plotted against target concentration.

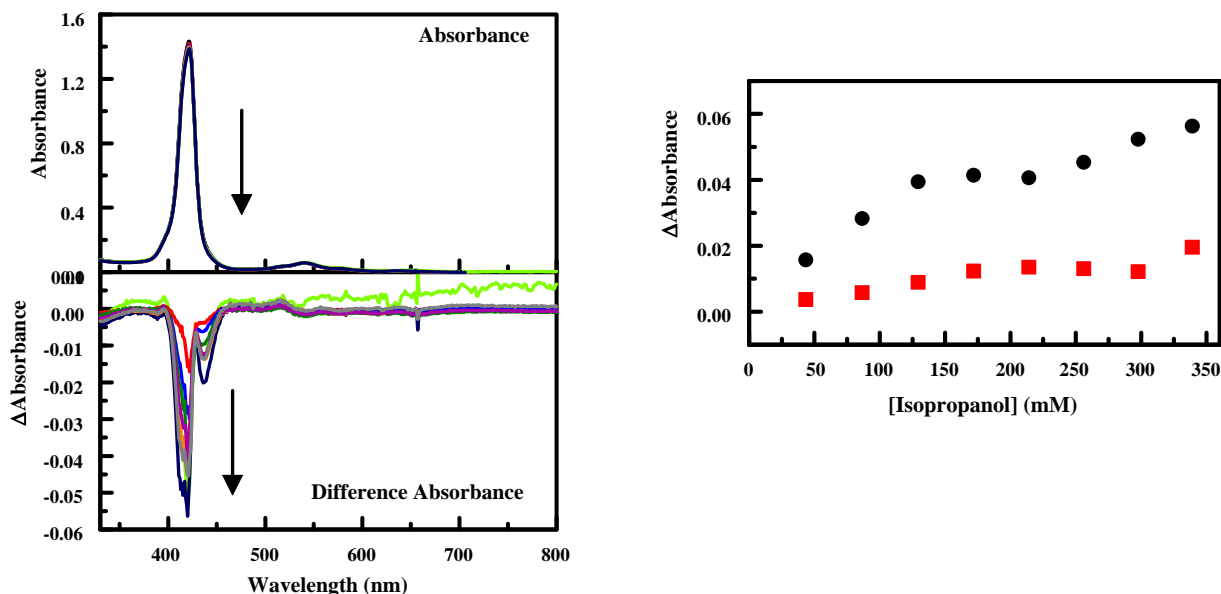


Figure A-6. Absorbance spectra (top) of AgC₄TPP (9.86 μ M) in the absence and presence of increasing concentrations of methanol: 82, 163, 244, 325, 404, 483, 563, and 641 mM. Arrows indicate increasing target concentration. Absorbance spectra have been corrected for dilution resulting from target addition. Difference absorbance spectra (bottom) are calculated as porphyrin + target minus porphyrin. The concentration dependence of features in the absorbance spectra is also presented (right). Here, the change in absorbance at the trough positions (420 and 440 nm) is plotted against target concentration.

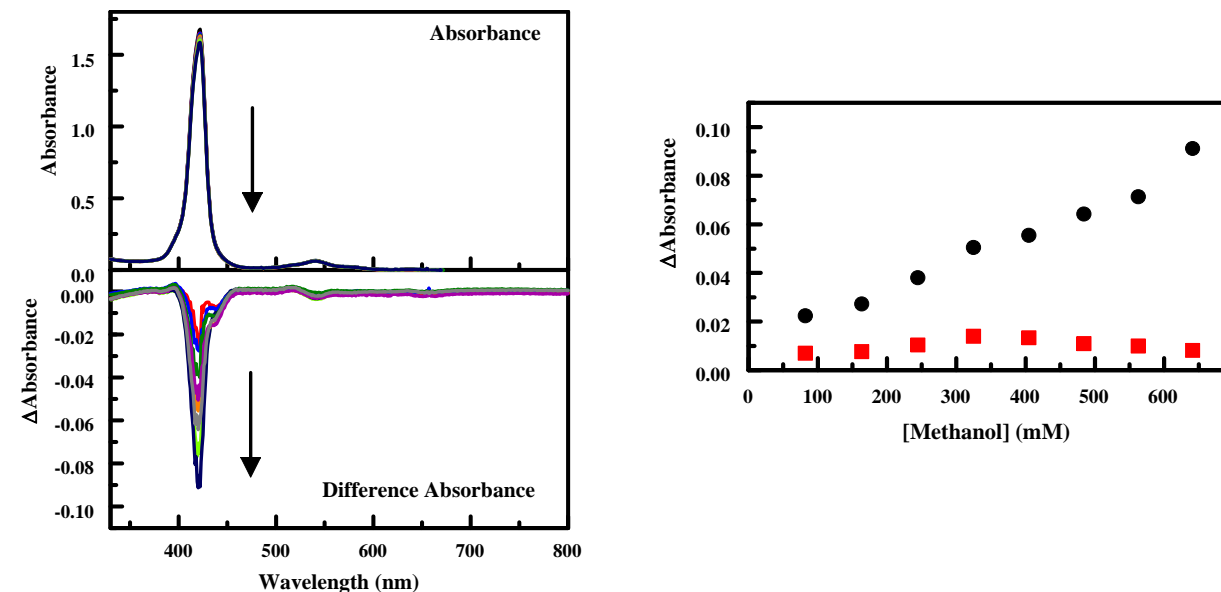


Figure A-7. Absorbance spectra (top) of CdC₄TPP (9.86 μ M) in the absence and presence of increasing concentrations of ethanol: 57, 113, 169, 225, 280, 335, 390, and 444 mM. Arrows indicate increasing target concentration. Absorbance spectra have been corrected for dilution resulting from target addition. Difference absorbance spectra (bottom) are calculated as porphyrin + target minus porphyrin. No specific changes in absorbance were noted.

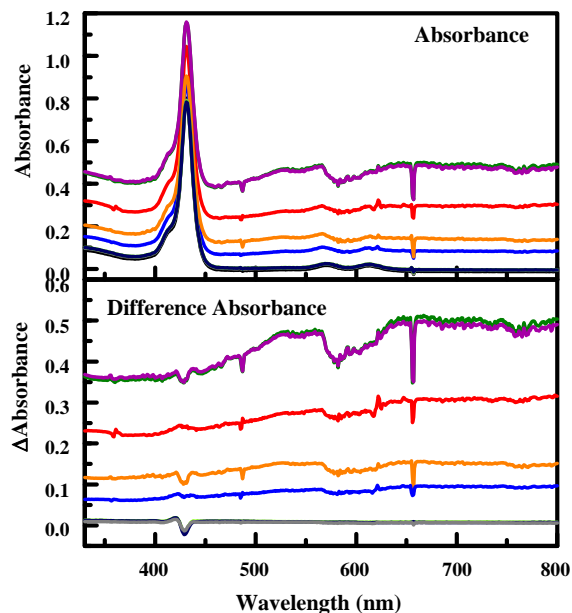


Figure A-8. Absorbance spectra (top) of CdC₄TPP (9.86 μ M) in the absence and presence of increasing concentrations of isopropanol: 43, 86, 129, 171, 214, 256, 298, and 339 mM. Arrows indicate increasing target concentration. Absorbance spectra have been corrected for dilution resulting from target addition. Difference absorbance spectra (bottom) are calculated as porphyrin + target minus porphyrin. The concentration dependence of features in the absorbance spectra is also presented (right). Here, the change in absorbance at the trough positions (408 and 430 nm) is plotted against target concentration.

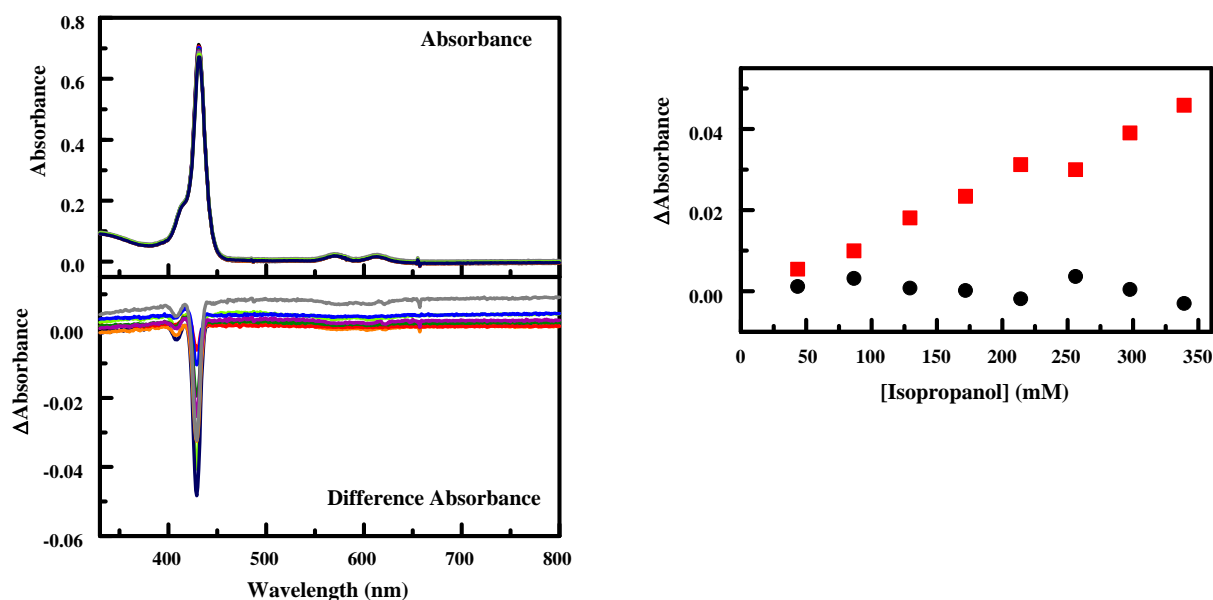


Figure A-9. Absorbance spectra (top) of CdC₄TPP (9.86 μ M) in the absence and presence of increasing concentrations of methanol: 82, 163, 244, 325, 404, 483, 563, and 641 mM. Arrows indicate increasing target concentration. Absorbance spectra have been corrected for dilution resulting from target addition. Difference absorbance spectra (bottom) are calculated as porphyrin + target minus porphyrin. The concentration dependence of features in the absorbance spectra is also presented (right). Here, the change in absorbance at the trough positions (408 and 430 nm) is plotted against target concentration.

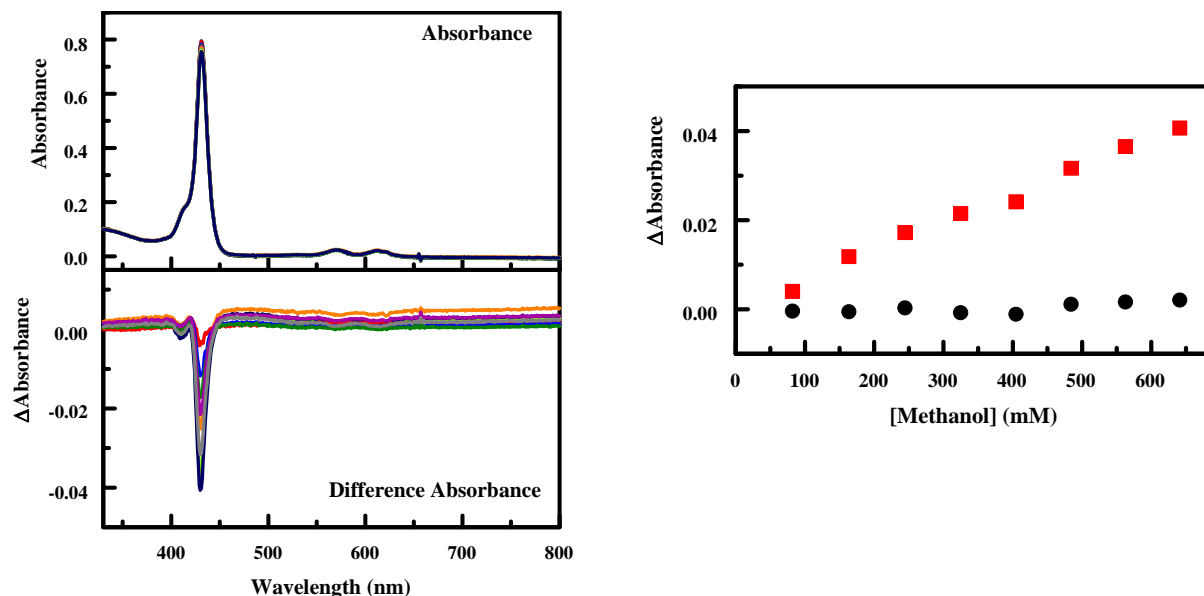


Figure A-10. Absorbance spectra (top) of CeC₄TPP (9.86 μ M) in the absence and presence of increasing concentrations of ethanol: 57, 113, 169, 225, 280, 335, 390, and 444 mM. Arrows indicate increasing target concentration. Absorbance spectra have been corrected for dilution resulting from target addition. Difference absorbance spectra (bottom) are calculated as porphyrin + target minus porphyrin. The concentration dependence of features in the absorbance spectra is also presented (right). Here, the change in absorbance at the trough and peak positions (408 and 422 nm) is plotted against target concentration.

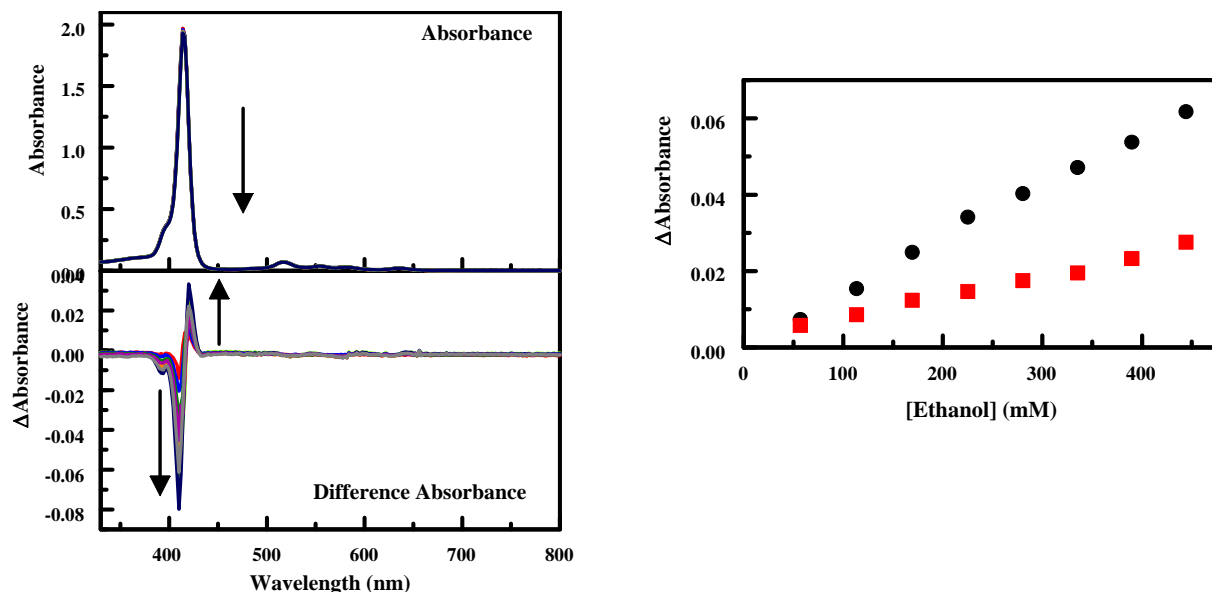


Figure A-11. Absorbance spectra (top) of CeC₄TPP (9.86 μ M) in the absence and presence of increasing concentrations of isopropanol: 43, 86, 129, 171, 214, 256, 298, and 339 mM. Arrows indicate increasing target concentration. Absorbance spectra have been corrected for dilution resulting from target addition. Difference absorbance spectra (bottom) are calculated as porphyrin + target minus porphyrin. The concentration dependence of features in the absorbance spectra is also presented (right). Here, the change in absorbance at the trough and peak positions (411 and 424 nm) is plotted against target concentration.

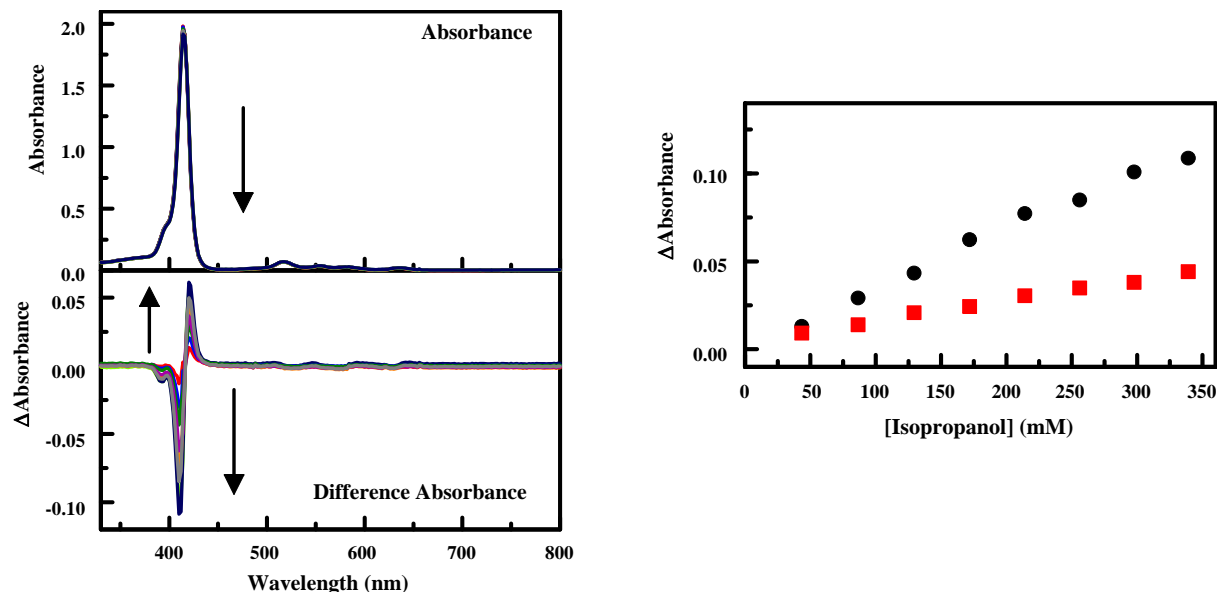


Figure A-12. Absorbance spectra (top) of CeC₄TPP (9.86 μ M) in the absence and presence of increasing concentrations of methanol: 82, 163, 244, 325, 404, 483, 563, and 641 mM. Arrows indicate increasing target concentration. Absorbance spectra have been corrected for dilution resulting from target addition. Difference absorbance spectra (bottom) are calculated as porphyrin + target minus porphyrin. The concentration dependence of features in the absorbance spectra is also presented (right). Here, the change in absorbance at the trough and peak positions (410 and 420 nm) is plotted against target concentration.

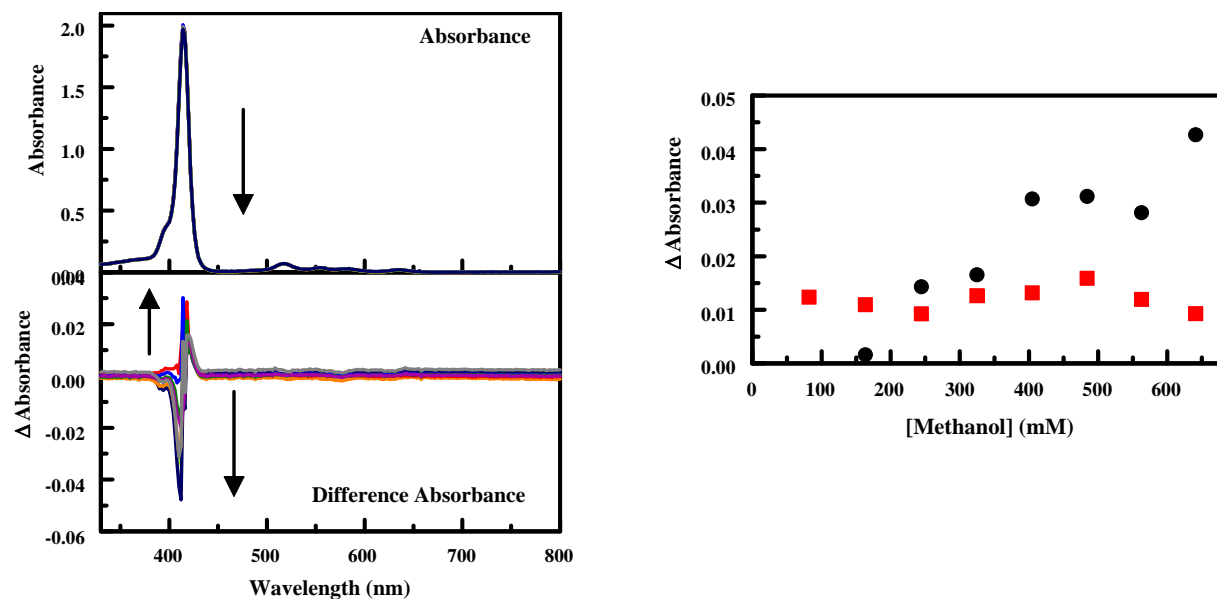


Figure A-13. Absorbance spectra (top) of CoC₄TPP (9.86 μ M) in the absence and presence of increasing concentrations of ethanol: 57, 113, 169, 225, 280, 335, 390, and 444 mM. Arrows indicate increasing target concentration. Absorbance spectra have been corrected for dilution resulting from target addition. Difference absorbance spectra (bottom) are calculated as porphyrin + target minus porphyrin. The concentration dependence of features in the absorbance spectra is also presented (right). Here, the change in absorbance at the trough and peak positions (412 and 420 nm) is plotted against target concentration.

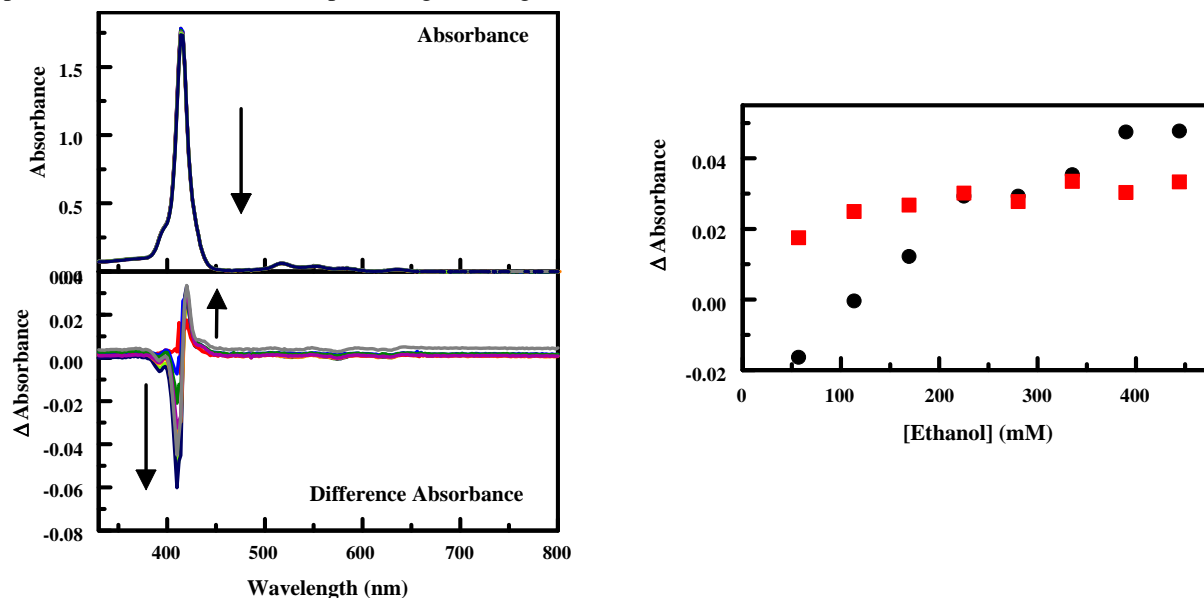


Figure A-14. Absorbance spectra (top) of CoC₄TPP (9.86 μ M) in the absence and presence of increasing concentrations of isopropanol: 43, 86, 129, 171, 214, 256, 298, and 339 mM. Arrows indicate increasing target concentration. Absorbance spectra have been corrected for dilution resulting from target addition. Difference absorbance spectra (bottom) are calculated as porphyrin + target minus porphyrin. The concentration dependence of features in the absorbance spectra is also presented (right). Here, the change in absorbance at the trough and peak positions (410 and 422 nm) is plotted against target concentration.

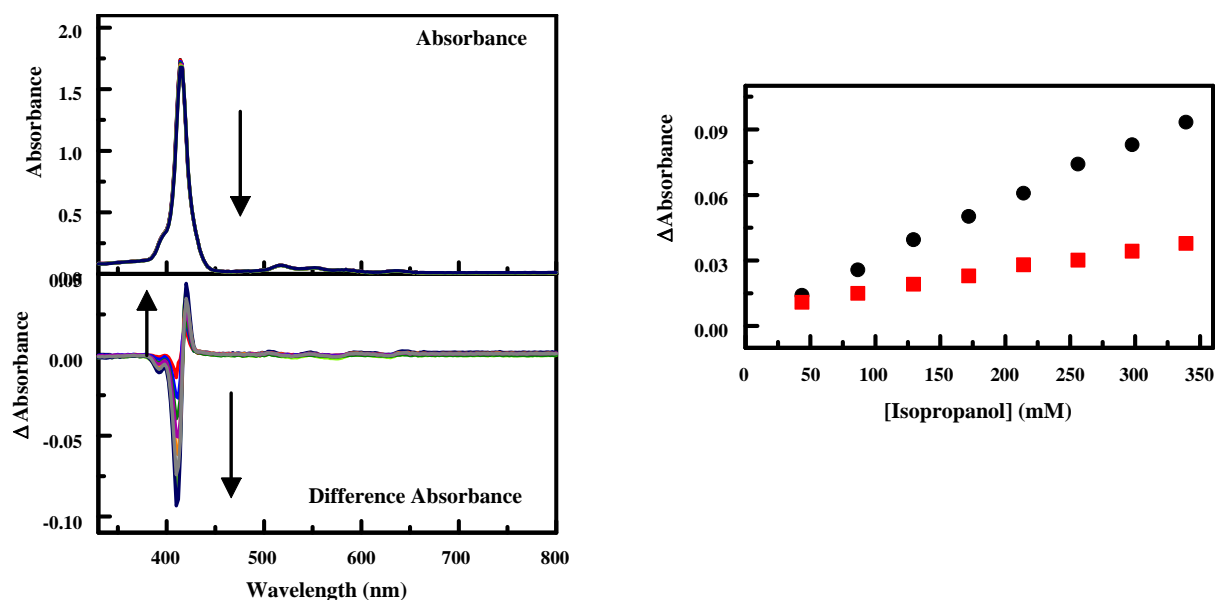


Figure A-15. Absorbance spectra (top) of CoC₄TPP (9.86 μ M) in the absence and presence of increasing concentrations of methanol: 82, 163, 244, 325, 404, 483, 563, and 641 mM. Arrows indicate increasing target concentration. Absorbance spectra have been corrected for dilution resulting from target addition. Difference absorbance spectra (bottom) are calculated as porphyrin + target minus porphyrin. The concentration dependence of features in the absorbance spectra is also presented (right). Here, the change in absorbance at the trough and peak positions (412 and 422 nm) is plotted against target concentration.

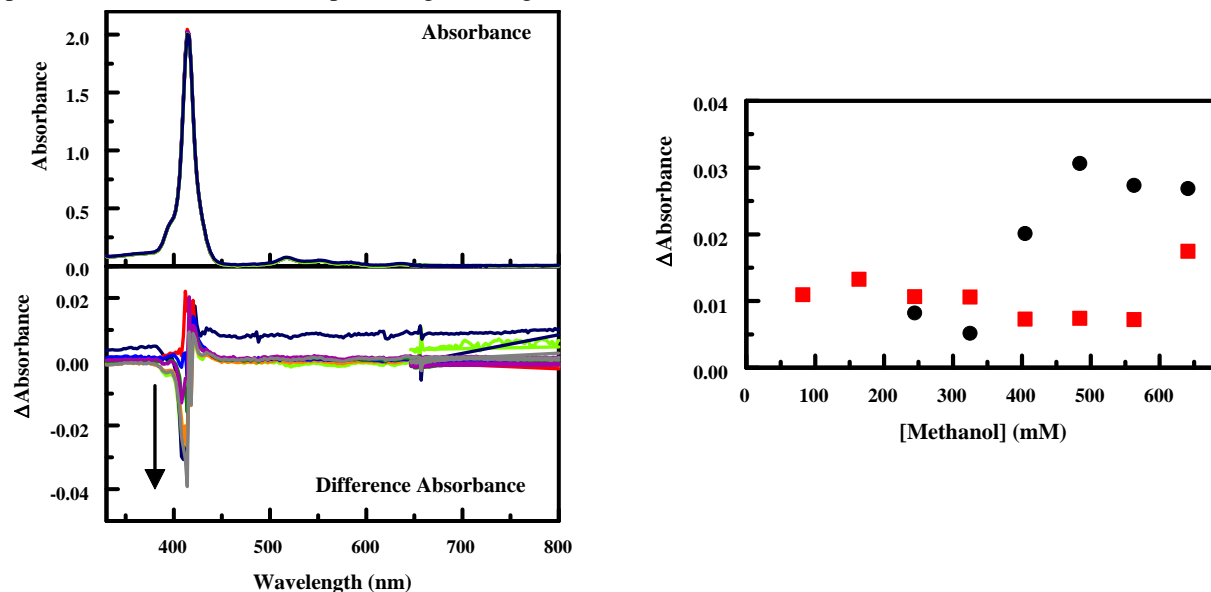


Figure A-16. Absorbance spectra (top) of CuC₄TPP (9.86 μ M) in the absence and presence of increasing concentrations of ethanol: 57, 113, 169, 225, 280, 335, 390, and 444 mM. Arrows indicate increasing target concentration. Absorbance spectra have been corrected for dilution resulting from target addition. Difference absorbance spectra (bottom) are calculated as porphyrin + target minus porphyrin. The concentration dependence of features in the absorbance spectra is also presented (right). Here, the change in absorbance at the trough positions (404 and 414 nm) is plotted against target concentration.

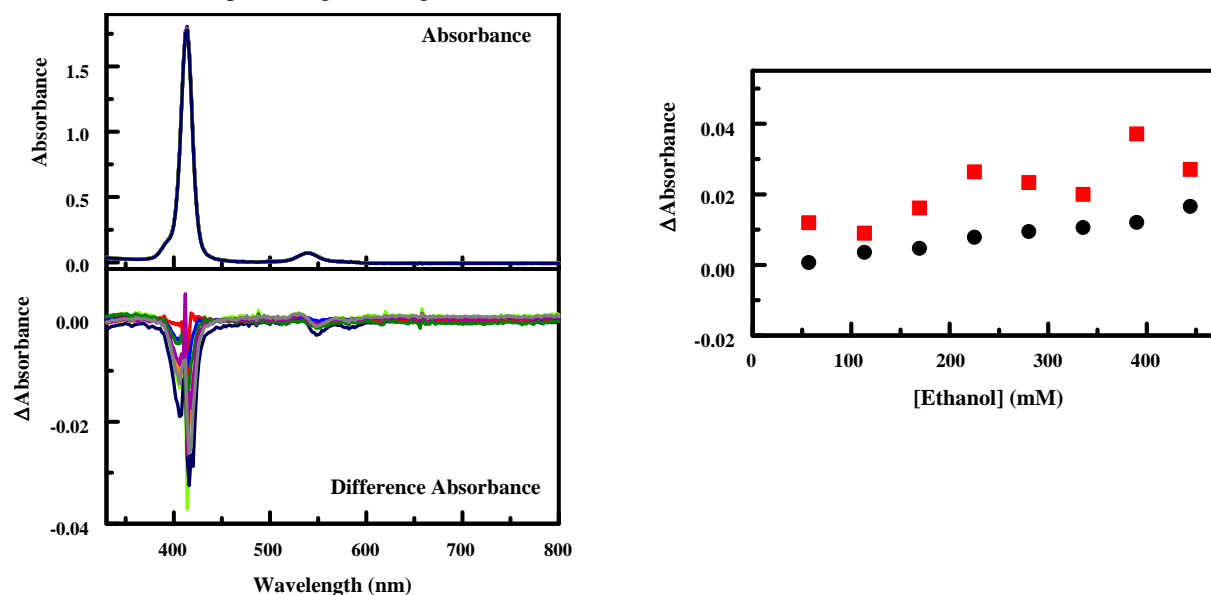


Figure A-17. Absorbance spectra (top) of CuC₄TPP (9.86 μ M) in the absence and presence of increasing concentrations of isopropanol: 43, 86, 129, 171, 214, 256, 298, and 339 mM. Arrows indicate increasing target concentration. Absorbance spectra have been corrected for dilution resulting from target addition. Difference absorbance spectra (bottom) are calculated as porphyrin + target minus porphyrin. The concentration dependence of features in the absorbance spectra is also presented (right). Here, the change in absorbance at the trough positions (402 and 420 nm) is plotted against target concentration.

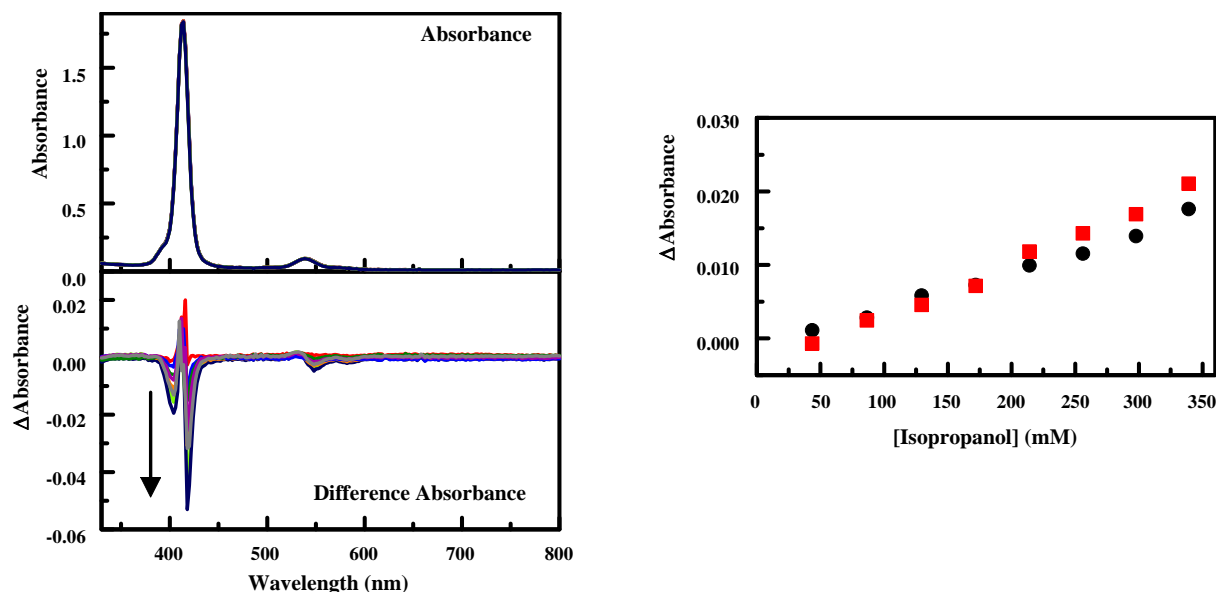


Figure A-18. Absorbance spectra (top) of CuC₄TPP (9.86 μ M) in the absence and presence of increasing concentrations of methanol: 82, 163, 244, 325, 404, 483, 563, and 641 mM. Arrows indicate increasing target concentration. Absorbance spectra have been corrected for dilution resulting from target addition. Difference absorbance spectra (bottom) are calculated as porphyrin + target minus porphyrin. The concentration dependence of features in the absorbance spectra is also presented (right). Here, the change in absorbance at the trough positions (406 and 422 nm) is plotted against target concentration.

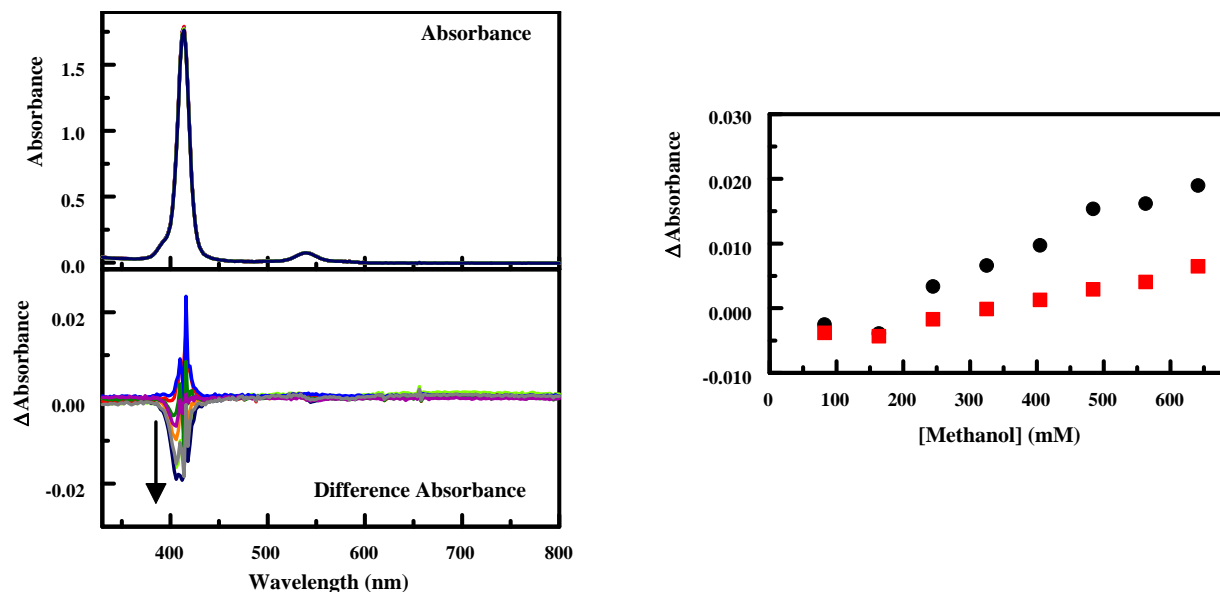


Figure A-19. Absorbance spectra (top) of FeC₄TPP (9.86 μ M) in the absence and presence of increasing concentrations of ethanol: 57, 113, 169, 225, 280, 335, 390, and 444 mM. Arrows indicate increasing target concentration. Absorbance spectra have been corrected for dilution resulting from target addition. Difference absorbance spectra (bottom) are calculated as porphyrin + target minus porphyrin. The concentration dependence of features in the absorbance spectra is also presented (right). Here, the change in absorbance at the trough and peak positions (408 and 424 nm) is plotted against target concentration.

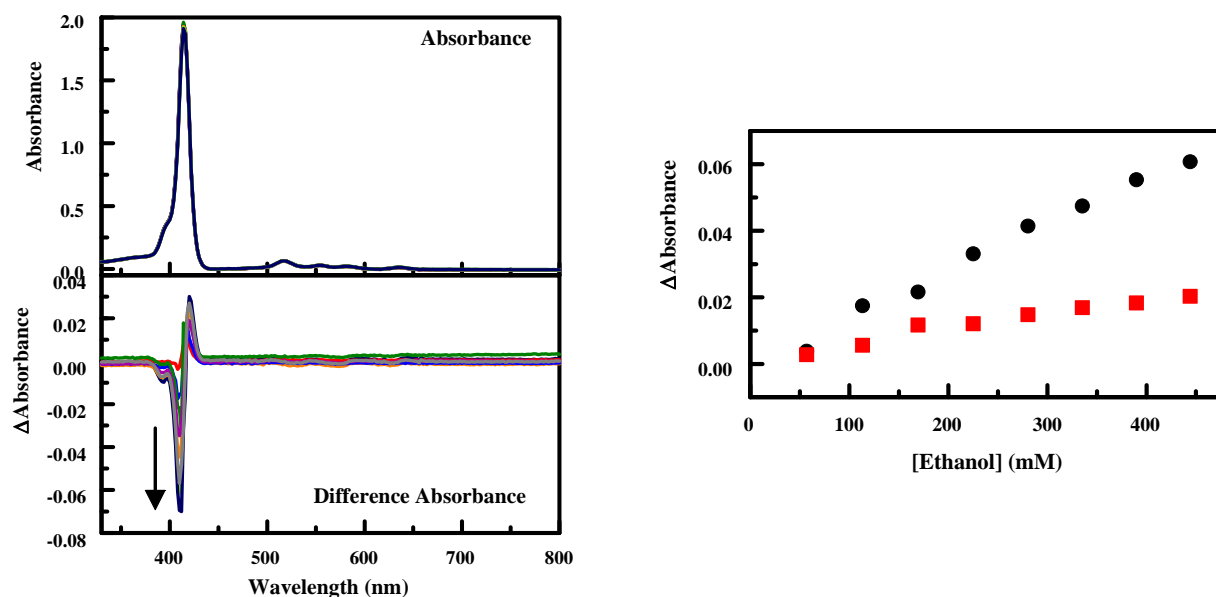


Figure A-20. Absorbance spectra (top) of FeC₄TPP (9.86 μ M) in the absence and presence of increasing concentrations of isopropanol: 43, 86, 129, 171, 214, 256, 298, and 339 mM. Arrows indicate increasing target concentration. Absorbance spectra have been corrected for dilution resulting from target addition. Difference absorbance spectra (bottom) are calculated as porphyrin + target minus porphyrin. The concentration dependence of features in the absorbance spectra is also presented (right). Here, the change in absorbance at the trough and peak positions (410 and 420 nm) is plotted against target concentration.

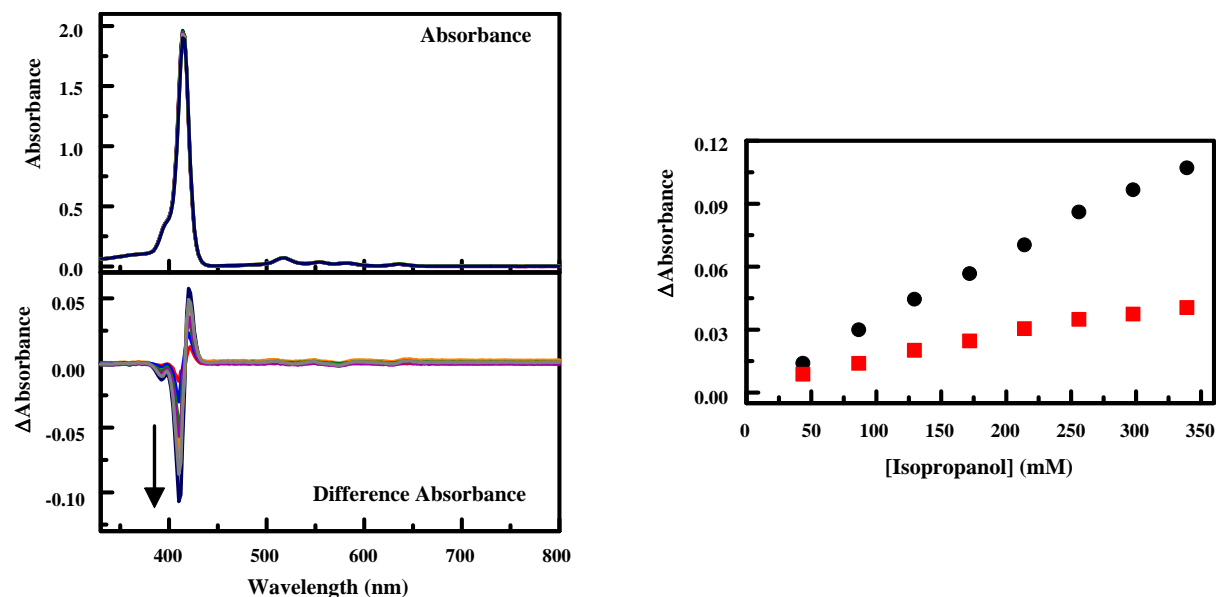


Figure A-21. Absorbance spectra (top) of FeC₄TPP (9.86 μ M) in the absence and presence of increasing concentrations of methanol: 82, 163, 244, 325, 404, 483, 563, and 641 mM. Arrows indicate increasing target concentration. Absorbance spectra have been corrected for dilution resulting from target addition. Difference absorbance spectra (bottom) are calculated as porphyrin + target minus porphyrin. The concentration dependence of features in the absorbance spectra is also presented (right). Here, the change in absorbance at the trough and peak positions (412 and 422 nm) is plotted against target concentration.

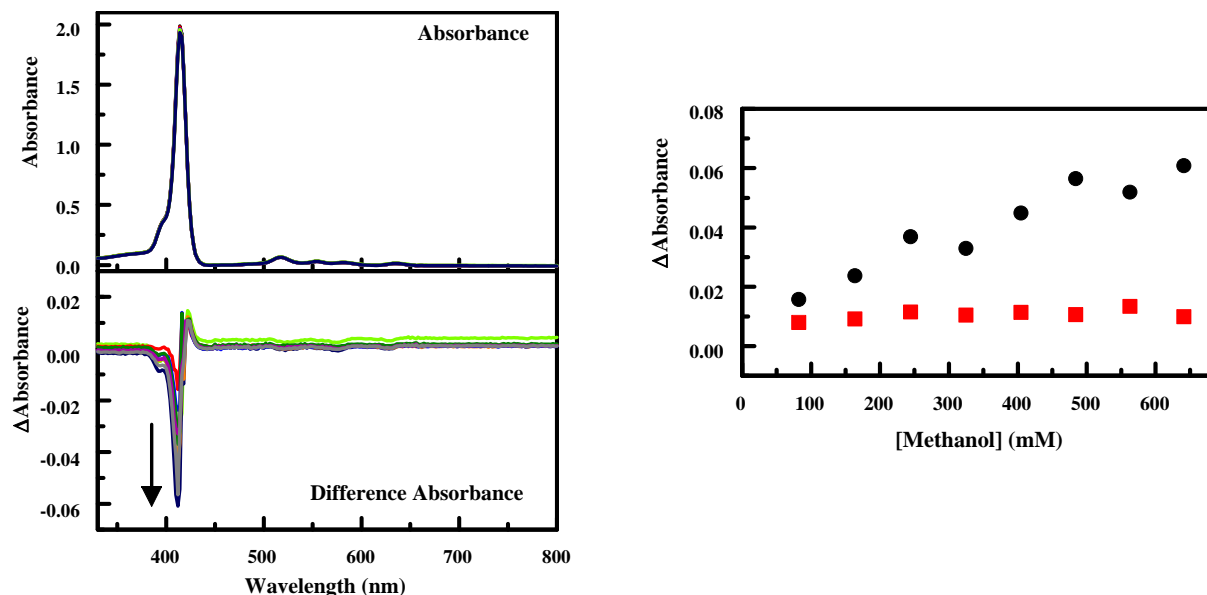


Figure A-22. Absorbance spectra (top) of NiC₄TPP (9.86 μ M) in the absence and presence of increasing concentrations of ethanol: 57, 113, 169, 225, 280, 335, 390, and 444 mM. Arrows indicate increasing target concentration. Absorbance spectra have been corrected for dilution resulting from target addition. Difference absorbance spectra (bottom) are calculated as porphyrin + target minus porphyrin. The concentration dependence of features in the absorbance spectra is also presented (right). Here, the change in absorbance at the trough and peak positions (407 and 421 nm) is plotted against target concentration.

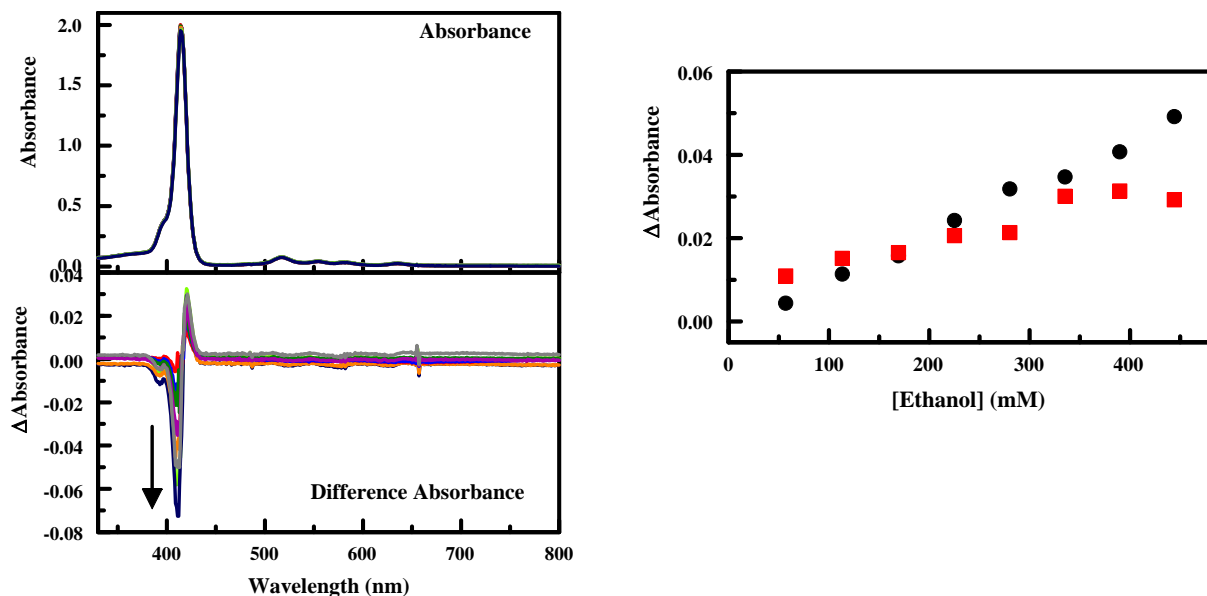


Figure A-23. Absorbance spectra (top) of NiC₄TPP (9.86 μ M) in the absence and presence of increasing concentrations of isopropanol: 43, 86, 129, 171, 214, 256, 298, and 339 mM. Arrows indicate increasing target concentration. Absorbance spectra have been corrected for dilution resulting from target addition. Difference absorbance spectra (bottom) are calculated as porphyrin + target minus porphyrin. The concentration dependence of features in the absorbance spectra is also presented (right). Here, the change in absorbance at the trough and peak positions (411 and 422 nm) is plotted against target concentration.

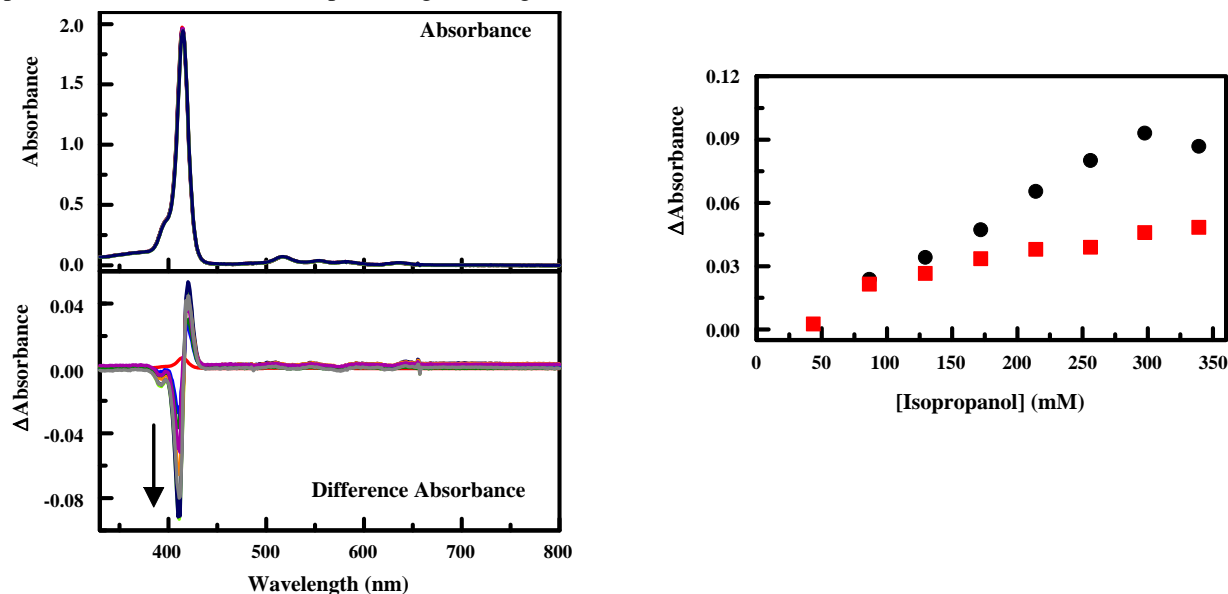


Figure A-24. Absorbance spectra (top) of NiC₄TPP (9.86 μ M) in the absence and presence of increasing concentrations of methanol: 82, 163, 244, 325, 404, 483, 563, and 641 mM. Arrows indicate increasing target concentration. Absorbance spectra have been corrected for dilution resulting from target addition. Difference absorbance spectra (bottom) are calculated as porphyrin + target minus porphyrin. The concentration dependence of features in the absorbance spectra is also presented (right). Here, the change in absorbance at the trough positions (392 and 414 nm) is plotted against target concentration.

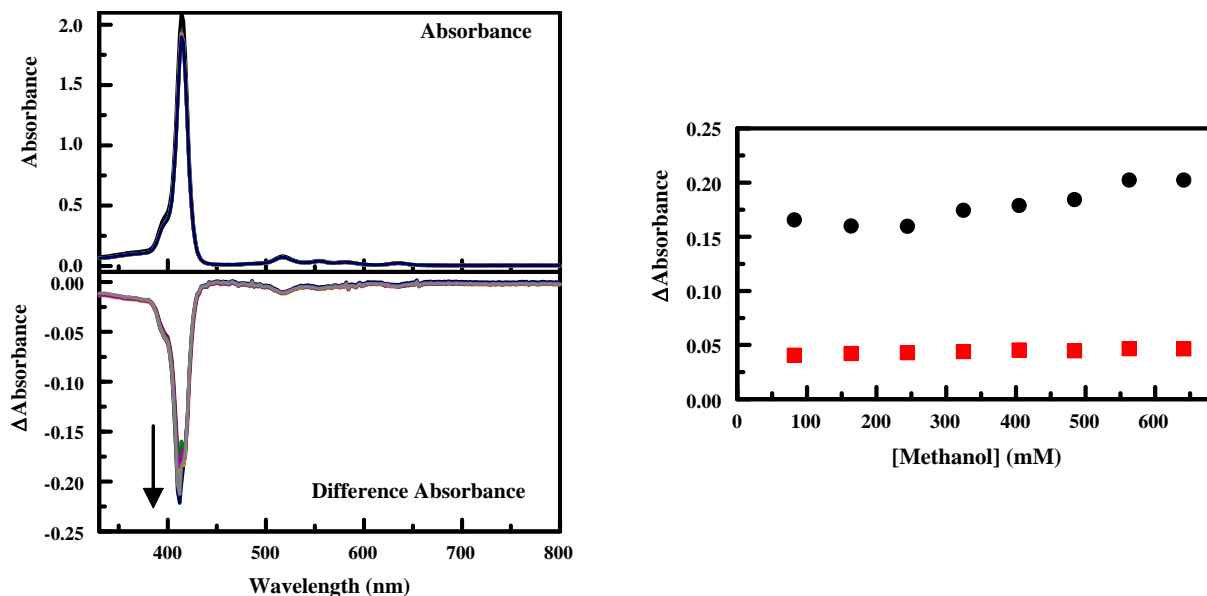


Figure A-25. Absorbance spectra (top) of YC₄TPP (9.86 μ M) in the absence and presence of increasing concentrations of ethanol: 57, 113, 169, 225, 280, 335, 390, and 444 mM. Arrows indicate increasing target concentration. Absorbance spectra have been corrected for dilution resulting from target addition. Difference absorbance spectra (bottom) are calculated as porphyrin + target minus porphyrin. The concentration dependence of features in the absorbance spectra is also presented (right). Here, the change in absorbance at the trough and peak positions (411 and 436 nm) is plotted against target concentration.

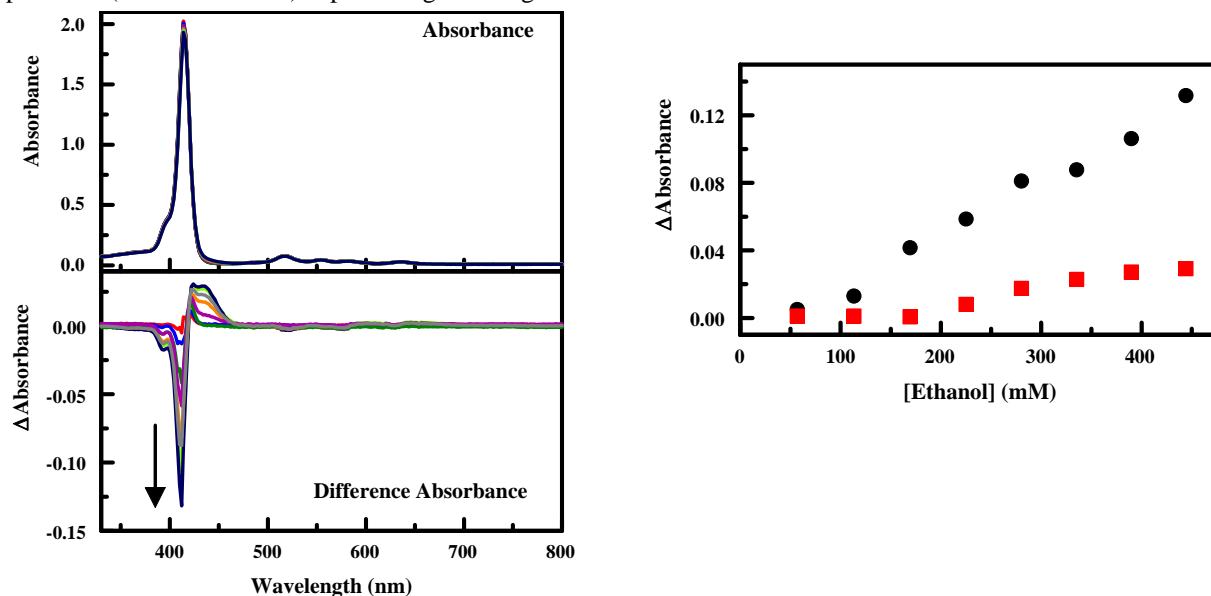


Figure A-26. Absorbance spectra (top) of YC₄TPP (9.86 μ M) in the absence and presence of increasing concentrations of isopropanol: 43, 86, 129, 171, 214, 256, 298, and 339 mM. Arrows indicate increasing target concentration. Absorbance spectra have been corrected for dilution resulting from target addition. Difference absorbance spectra (bottom) are calculated as porphyrin + target minus porphyrin. The concentration dependence of features in the absorbance spectra is also presented (right). Here, the change in absorbance at the trough and peak positions (412 and 420 nm) is plotted against target concentration.

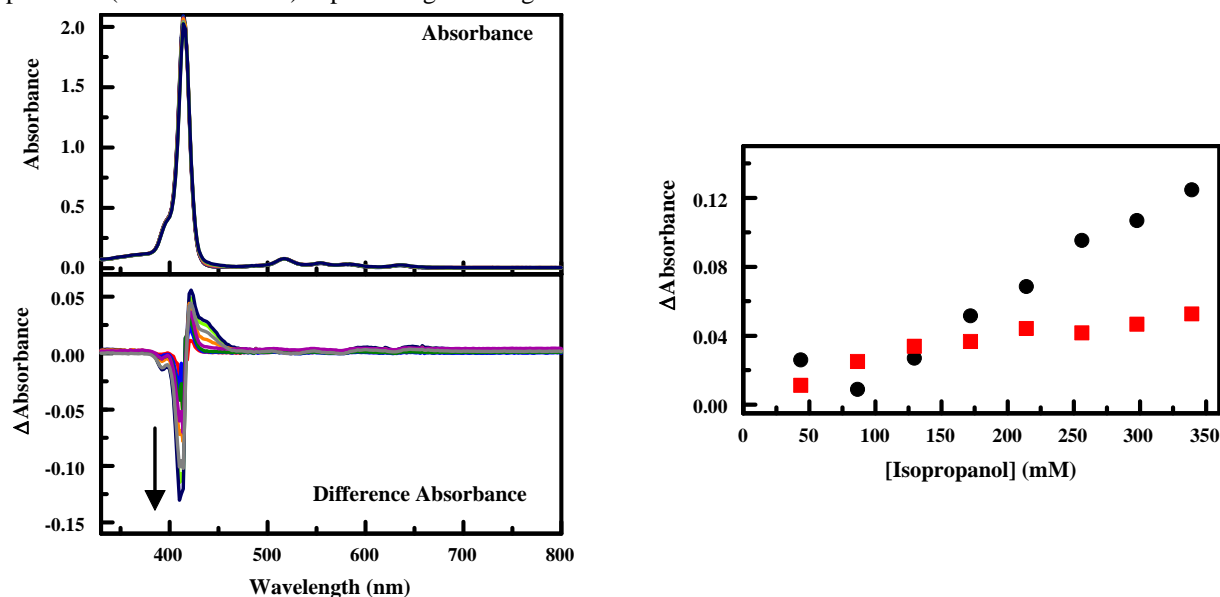


Figure A-27. Absorbance spectra (top) of YC₄TPP (9.86 μ M) in the absence and presence of increasing concentrations of methanol: 82, 163, 244, 325, 404, 483, 563, and 641 mM. Arrows indicate increasing target concentration. Absorbance spectra have been corrected for dilution resulting from target addition. Difference absorbance spectra (bottom) are calculated as porphyrin + target minus porphyrin. The concentration dependence of features in the absorbance spectra is also presented (right). Here, the change in absorbance at the trough positions (410 and 426 nm) is plotted against target concentration.

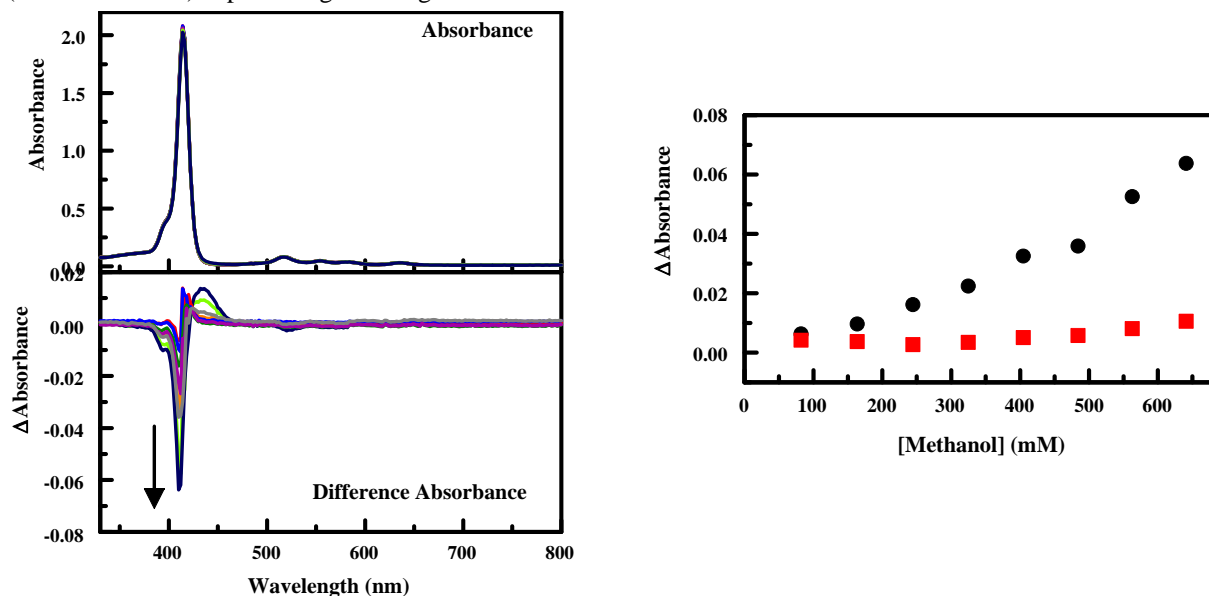


Figure A-28. Absorbance spectra (top) of ZnC₄TPP (9.86 μ M) in the absence and presence of increasing concentrations of ethanol: 57, 113, 169, 225, 280, 335, 390, and 444 mM. Arrows indicate increasing target concentration. Absorbance spectra have been corrected for dilution resulting from target addition. Difference absorbance spectra (bottom) are calculated as porphyrin + target minus porphyrin. The concentration dependence of features in the absorbance spectra is also presented (right). Here, the change in absorbance at the trough positions (388 and 422 nm) is plotted against target concentration.

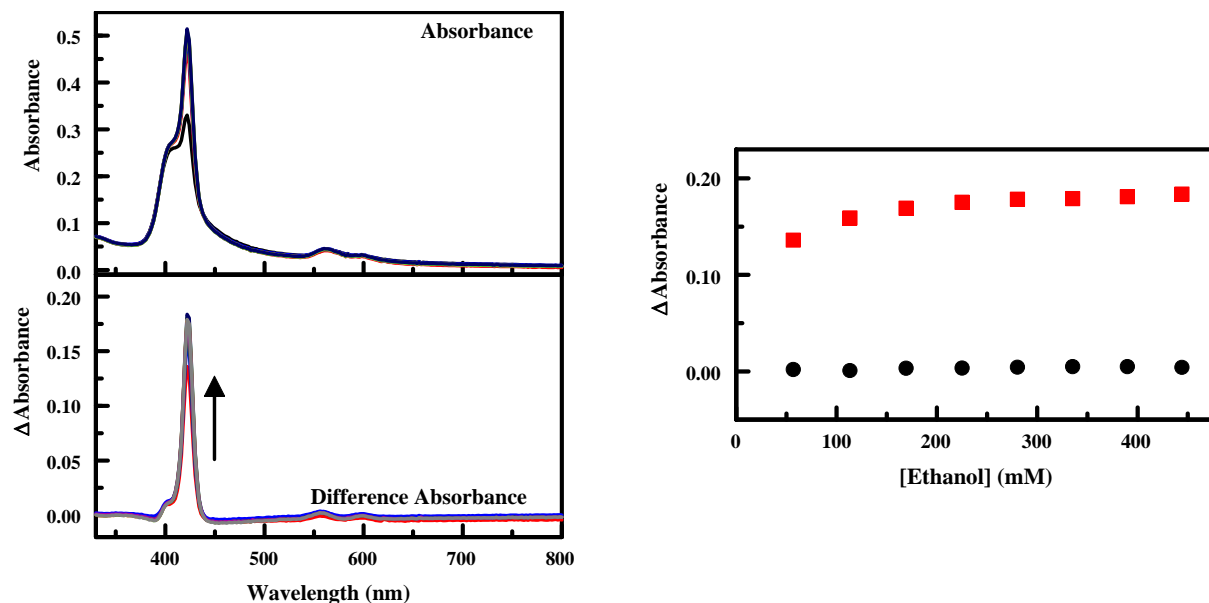


Figure A-29. Absorbance spectra (top) of ZnC_4TPP ($9.86 \mu\text{M}$) in the absence and presence of increasing concentrations of isopropanol: 43, 86, 129, 171, 214, 256, 298, and 339 mM. Arrows indicate increasing target concentration. Absorbance spectra have been corrected for dilution resulting from target addition. Difference absorbance spectra (bottom) are calculated as porphyrin + target minus porphyrin. The concentration dependence of features in the absorbance spectra is also presented (right). Here, the change in absorbance at the trough and peak positions (390 and 424 nm) is plotted against target concentration.

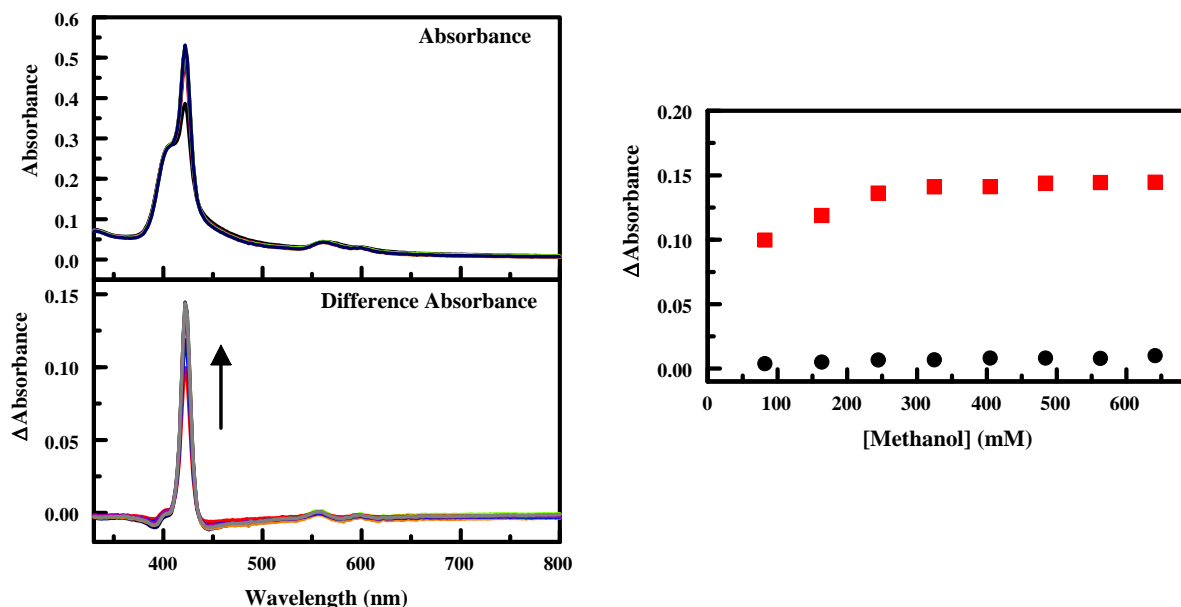


Figure A-30. Absorbance spectra (top) of ZnC_4TPP ($9.86 \mu\text{M}$) in the absence and presence of increasing concentrations of methanol: 82, 163, 244, 325, 404, 483, 563, and 641 mM. Arrows indicate increasing target concentration. Absorbance spectra have been corrected for dilution resulting from target addition. Difference absorbance spectra (bottom) are calculated as porphyrin + target minus porphyrin. The concentration dependence of features in the absorbance spectra is also presented (right). Here, the change in absorbance at the trough and peak positions (390 and 424 nm) is plotted against target concentration.

